Laser and Particle Beams (2004), *22*, 215–220. Printed in the USA.

DOI: 10.1017/S0263034604223047

Generation of X rays and energetic ions from superintense laser irradiation of micron-sized Ar clusters

Y. FUKUDA,[1] Y. AKAHANE,[1] M. AOYAMA,[1] N. INOUE,[1] H. UEDA,[1] Y. KISHIMOTO,[2] K. YAMAKAWA,[1] A.YA. FAENOV,[3] A.I. MAGUNOV,[3] T.A. PIKUZ,[3] I.YU. SKOBELEV,[3] J. ABDALLAH, JR.,[4] G. CSANAK,[4] A.S. BOLDAREV,[5] AND V.A. GASILOV[5]

[1]Advanced Photon Research Center, Japan Atomic Energy Research Institute, Kizu-cho, Kyoto, Japan
[2]Naka Fusion Research Establishment, Japan Atomic Energy Research Institute, Naka, Ibaraki, Japan
[3]Multicharged Ions Spectra Data Center of VNIIFTRI, Mendeleevo, Moscow, Russia
[4]Theoretical Division, Los Alamos National Laboratory, Los Alamos, NM
[5]Institute of Mathematical Modeling, Russian Academy of Sciences, Moscow, Russia

(RECEIVED 1 November 2003; ACCEPTED 17 February 2004)

Abstract

High-resolution *K*-shell spectra of a plasma created by superintense laser irradiation of micron-sized Ar clusters have been measured with an intensity above 10^{19} W/cm^2 and a pulse duration of 30 fs. The total photon flux of 2×10^8 photons/pulse was achieved for $He_{\alpha 1}$ resonant line of Ar (λ = 3.9491 Å, 3.14 keV). In parallel with X-ray measurements, energy distributions of emitted ions have been measured. The multiply charged ions with kinetic energies up to 800 keV were observed. It is found that hot electrons produced by high contrast laser pulses allow the isochoric heating of clusters and shift the ion balance toward the higher charge states, which enhances both the X-ray line yield of the He-like argon ion and the ion kinetic energy.

Keywords: Cluster; High power laser; Isochoric heating; Multiply charged ion; X ray

1. INTRODUCTION

Recent development of ultrashort, high peak-power laser systems, based on the chirped pulse amplification (CPA) technique, opens up a new regime of laser–matter interaction (Perry & Mourou, 1994). Nowadays a focusing of such laser pulses produces laser peak intensities well above 10^{19} W/cm^2. One of important features of such an interaction is that a laser pulse duration is much shorter than the typical time scale of hydrodynamic plasma expansion, which allows isochoric heating of matter, that is, a generation of hot plasmas at near solid density (Eidmann *et al.*, 2003). The heated region remains in the dense state for 1–2 ps before significant expansion begins. The previous study predicts that X-ray emission from plasmas characterized by overcritical densities occur on time scales comparable to the laser pulse duration, whereas emission from plasmas at or below critical density may last for times longer than the laser pulse duration (Junkel-Vives *et al.*, 2002).

Address correspondence and reprint requests to: Yuji Fukuda, Advanced Photon Research Center, Japan Atomic Energy Research Institute, Kizu-cho, Kyoto 619-0215, Japan. E-mail: fukuda@apr.jaeri.go.jp

The interactions of intense laser fields with clusters exhibit distinctive features from other targets (Posthumus, 2001). This is because the clusters absorb most of the incident laser energy, and the absorbed energy cannot dissipate due to the finite system of clusters. This heats up the clusters significantly and leads to a number of characteristic phenomena such as enhanced emissions of X rays in the kiloelectron volt range (McPherson *et al.*, 1994), generation of kiloelectron volt electrons and multiply charged ions with kinetic energies up to 1 MeV (Ditmire *et al.*, 1998), and nuclear-fusion events using collisions of fast ions from deuterium clusters (Ditmire *et al.*, 1999). They are expected to be utilized as a debris-free X-ray source for microscopy or lithography, an electron/ion source for a table-top accelerator, and an neutron source for a material damage study.

Achievement of isochoric heating in cluster media is a promising way to develop a debris-free ultrashort (fs–ps) intense X-ray source for time-resolved X-ray diffraction experiments. When a sufficiently short and intense laser pulse is used, the laser energy is deposited before the cluster can expand. However, to establish isochoric heating in superintense laser fields, we have to avoid a low-density

preplasma formation by a laser prepulse. The preplasma formation dramatically decreases X-ray emission yield. In this study, to suppress the preplasma formation, we eliminated the prepulse using Pockels cell switches. In addition, we tried to increase the cluster size using a specially designed conical nozzle, which could produce massive clusters with a diameter of ~ 1 μm. These approaches contribute to guaranteeing the direct interaction between the high-density cluster and the main fs pulse, and to establish isochoric heating.

To better understand a fundamental aspect of the laser–cluster interaction, we have in this article carried out systematic investigations of X-ray radiation properties of high-density and high-temperature cluster plasma, created by the action of superintense laser irradiation. Moreover, the interrelationship between the X-ray radiation properties and ion kinetic energies was examined by the simultaneous measurements of X-ray radiation spectra and ion energy spectra.

2. EXPERIMENTAL PROCEDURE

The experiments were performed with the JAERI (Kyoto, Japan) 100 TW Ti:sapphire laser system based on the technique of chirped pulse amplification, which was designed to generate 20-fs pulses centered at 800 nm at 10 Hz repetition rate and capable of producing focusing intensity up to 10^{20} W/cm^2 (Yamakawa *et al.*, 1998). In this study, the amplified pulses were compressed to 30 fs by a vacuum pulse compressor yielding a pulse energy up to 320 mJ. In this system, after the regenerative amplifier, the pulses go through two double Pockels cell switches to eliminate a prepulse, which comes before the main pulse by 10 ns. The laser pulse contrast achieved, that is, the ratio of the laser power in the maximum of the main femtosecond pulse to the prepulse power, was $C = 2 \times 10^5$. A schematic diagram of the experimental setup in JAERI is shown in Figure 1. In a vacuum target chamber, the compressed laser pulses were focused by an f/3 Au-coated off-axis parabolic mirror. The measured spot diameter was 11 μm at $1/e^2$ of the peak intensity, which was 1.1 times as large as that of the diffraction limit. Approximately 64% of the laser energy was contained in an 11-μm Gaussian spot. Ar clusters were produced by expanding a high-pressure ($p = 60$ bar) Ar gas into vacuum through a specially designed pulsed conical nozzle; the input and output diameters of the nozzle were 0.5 and 2.0 mm, respectively, and its length was 75 mm. The parameters of the nozzle were obtained from the numerical modeling of a cluster target using the code developed at the Institute of Mathematical Modeling (RAS; Dorchies *et al.*, 2003). By using this nozzle, the Ar clusters with an average diameter larger than 1 μm can be produced (Fukuda *et al.*, 2003*a*). The laser beam was focused about 1.5 mm downstream from the nozzle. The spatially resolved X-ray spectra were measured using a focusing spectrometer with spatial resolution (FSSR-2D; Blasco *et al.*, 2001). Such a spectrometer has been equipped with a spherically bent mica crystal ($R = 150$ mm) and a vacuum compatible X-ray CCD camera (DX420-BN, ANDOR). A spherically bent mica crystal has been placed at the distance of 381.2 mm from the plasma source and has been centered at $\lambda = 4.05$ Å, which corresponds to the Bragg angle $\theta = 54.3°$ for the fourth reflection order of the mica crystal. The reflection plane of the spectrometer was oriented along the direction of the laser beam propagation to obtain a spatial resolution in the transverse direction. The size of the emission zone in that direction was estimated as ~ 200 μm. In parallel with the X-ray measurements, the kinetic energies of the multiply charged ions, Ar^{n+}, ejected from the laser–cluster interaction region were measured by a time-of-flight (TOF) method. The 737-mm-long flight tube was oriented perpendicular to both the cluster beam and laser polarization axes. The ions fly through the field-free region, and are detected by a dual microchannel plates (MCP; F4655-12, Hamamatsu).

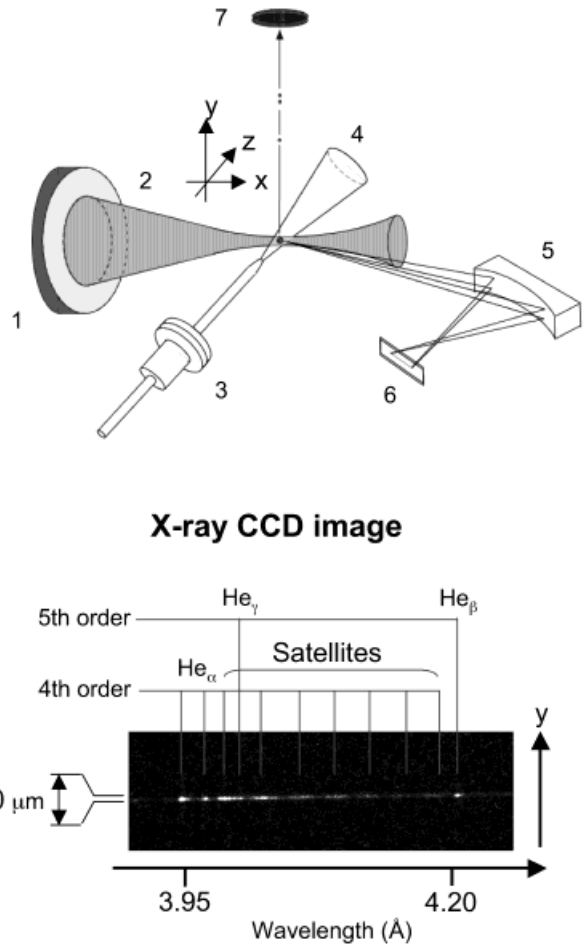

Fig. 1. A schematic diagram of the experimental setup: (1) the off-axis f/3 parabolic mirror, (2) the laser beam, (3) the specially designed pulsed conical nozzle, (4) the cluster gas jet, (5) the focusing spectrometer with the spherically bent mica crystal, (6) the vacuum compatible X-ray CCD camera, (7) the ion detector for TOF measurements.

https://doi.org/10.1017/S0263034604223047 Published online by Cambridge University Press

3. RESULTS AND DISCUSSION

3.1. X-ray emission spectra

Figure 2 shows the plasma emission spectrum measured at the Ar gas pressure of 60 bar with a laser intensity of 1.3×10^{19} W/cm^2, a pulse duration of 30 fs, and a laser contrast of 2×10^5. This spectrum was accumulated for 600 laser shots. The resonant ($He_{\alpha 1}$) and intercombination ($He_{\alpha 2}$) lines of the $1s2p$–$1s^2$ transition in the He-like argon ions are observed in the fourth reflection order as well as the clearly resolved structure of the dielectronic satellite lines in the Li-like argon ion and radiation lines from the autoionizing states $1s2s^m2p^n$ of the lower charged Be-like to F-like argon ions. The lines $1snp$–$1s^2$ ($n = 3$–6) in the He-like argon ion are observed in the fifth order at the same spectral record together with the dielectronic satellites of the $1s3p$–$1s^2$ line. Note that only a small amount of K_α emission (4.1947 Å) was observable in this experiment.

From the relative intensity of $He_{\alpha 1}$ and $He_{\alpha 2}$ lines, the plasma electron density was estimated as $N_e \sim 2 \times 10^{22}$ cm^{-3} (Junkel-Vives *et al.*, 2002). Note that this density is about 10 times greater than that of the critical density for Ti:sapphire lasers ($N_{crit} = 1.7 \times 10^{21}$ cm^{-3}), indicating that isochoric heating of the cluster target was established. The X-ray radiation from such an overcritically dense plasma is expected to be an ultrashort (fs–ps) X-ray source. According to a calculation based on a time-dependent Boltzmann-kinetic model, a pulse duration of a $He_{\alpha 1}$ line is estimated as ~3 ps (Abdallah *et al.*, 2004). The pulse duration measurement for generated X rays is now in progress. The number of photons N_{phot} in a 4π sr solid angle for $He_{\alpha 1}$ resonance line of Ar ($\lambda = 3.9491$ Å, 3.14 keV) was estimated by assuming a symmetric emission of X rays using the relation

$$N_{phot} = \frac{4\pi}{\Omega}\left(\frac{3.65}{3.14 \times 10^3} N \cdot g_{CCD}\right) \times (t_{acq} \cdot f_{laser} \cdot \tau_{filt} \cdot \rho_{cryst} \cdot \rho_{CCD})^{-1},$$

where N is the number of CCD counts per pixel ($\Delta\lambda = 5.8 \times 10^{-4}$ Å), g_{CCD} is the CCD gain, t_{acq} the acquisition time, f_{laser} the repetition rate of the laser pulse, τ_{filt} the transmission of filters, ρ_{cryst} the crystal reflectivity, ρ_{CCD} the quantum efficiency of the CCD sensor, and $\Omega = \Delta x \Delta y / a^2$ the solid angle from the target that contains X-ray radiation. Here $\Delta x \Delta y$ is the size of the reflected zone on the crystal, a is the distance between target and crystal for the $He_{\alpha 1}$ line. In our experiment, $\Delta x = 0.032$ mm, $\Delta y = 3.4$ mm, $a = 376$ mm, $N = 7040$ electrons per pixel, $g_{CCD} = 7$ electrons per A/D, $t_{acq} = 60$ s, $f_{laser} = 10$ Hz, $\tau_{filt} = 0.8$, $\rho_{cryst} = 0.01$, $\rho_{CCD} = 0.92$, so N_{phot} is estimated as 2×10^8 photons/pulse.

Figure 3 shows the cluster size dependence of X-ray emission spectra. The top, middle, and bottom curves represent the spectra measured with a laser contrast of 3×10^3 at Ar gas pressure of 60, 50, and 40 bar, respectively. Note that no X ray was observable at the Ar gas

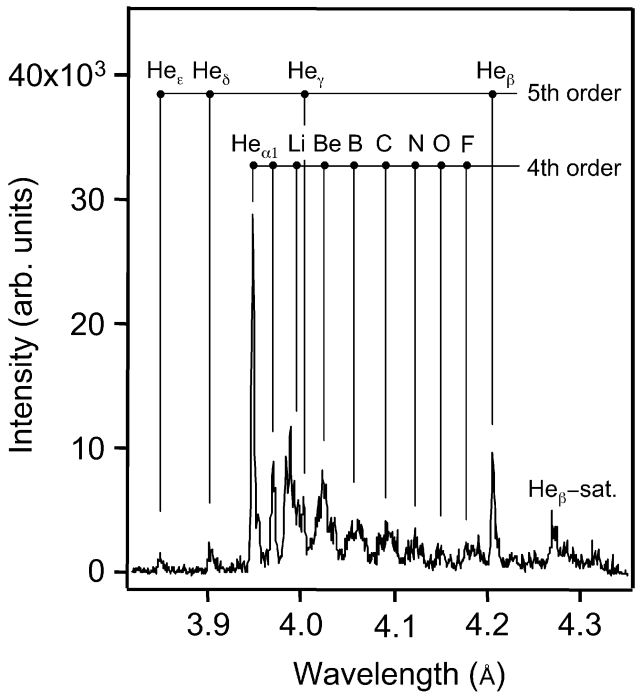

Fig. 2. The time-integrated X-ray emission spectrum of laser-irradiated micron-sized Ar clusters measured at an intensity of 1.2×10^{19} W/cm^2, a pulse duration of 30 fs, and a contrast ratio of 2×10^5.

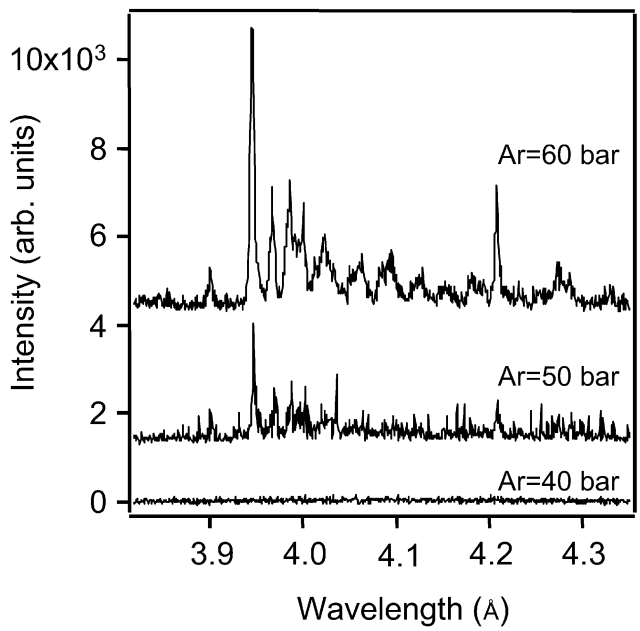

Fig. 3. The cluster size dependence of X-ray emission spectra measured at an intensity of 3×10^{18} W/cm^2, a pulse duration of 30 fs, and a laser contrast of 3×10^3: Ar = 60 bar (top curve); Ar = 50 bar (middle curve); Ar = 40 bar (bottom curve).

https://doi.org/10.1017/S0263034604223047 Published online by Cambridge University Press

pressure of 40 bar. According to the hydrodynamic calculation (Fukuda *et al.*, 2003*a*), at Ar = 40 bar the cluster size (average diameter of ~200 nm) is much smaller than that (average diameter of ~1 μm) for Ar = 60 bar. Thus, in the case of the 40-bar experiment, the prepulse could almost completely destroy the clusters. This result demonstrates the important role of large clusters, and the validity of the nozzle designing.

3.2. Ion energy spectra

To investigate interrelationship between X-ray emission properties and ion kinetic energy, in parallel with the X-ray measurements, the kinetic energies of the multiply charged ions, Ar^{n+}, emitted from the laser–cluster interaction region were measured using the TOF method. The ion energy spectrum was obtained by translating the TOF spectrum into an energy distribution function for the ions using the relation, $f(E) = f(t)(dE/dt)^{-1} = f(t)m_i^{-1}l^{-2}t^3$, where E is the ion kinetic energy, m_i the ion mass, l the length of the flight tube, and t the flight time. From the ion energy distribution function, the mean ion energy $\bar{E}_{ion}$, defined as $\bar{E}_{ion} = \int Ef(E)dE/\int f(E)dE$, was calculated. The uncertainties in the $\bar{E}_{ion}$ thus obtained are estimated to be less than ±2%. Figure 4 shows the typical ion energy spectrum obtained at a laser intensity of 3×10^{18} W/cm^2, a pulse duration of 30 fs, and a laser contrast of 2×10^5. The maximum ion energy observed is as high as E_{max} = 800 keV, and the mean ion energy was calculated as $\bar{E}_{ion}$ = 90 keV. The number of ions produced in a 4π sr solid angle with kinetic energies of 100 ± 1 keV is estimated as ~10^9 per pulse by taking account of the quantum efficiency and gain of the MCP detector and assuming a symmetric emission of energetic ions. Similar ion energy spectra are measured with different laser contrasts and pulse durations.

3.3. Interrelationship between X-ray emission properties and ion kinetic energies

The laser contrast dependence of X rays and ion energy spectra was investigated. Figure 5a shows the laser contrast dependence of X-ray spectra. The upper curve is obtained at an intensity of 3×10^{18} W/cm^2 and a laser contrast of 2×10^5. In this case, the intense resonance line ($He_{\alpha1}$) of He-like argon ions is observed. However, as shown in the lower curve, the observed spectrum changes dramatically with the change of the laser contrast from 2×10^5 (smaller prepulse) to 50 (greater prepulse): The line yield of He-like argon ions falls down significantly and X-ray emission from Be-like argon ions is dominant. This can be explained by the important role of laser prepulse. With the greater prepulse, the intensity of the prepulse is about 10^{16} W/cm^2. This is quite enough to ionize the clusters, and the main pulse interacts with a lower density preplasma. In this case, it is difficult to produce Ar ions with

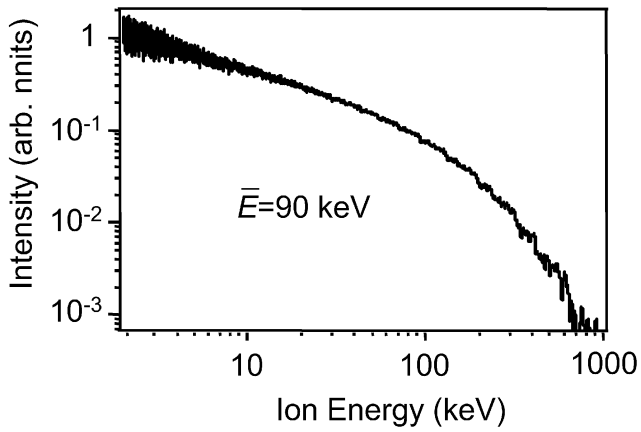

Fig. 4. Ion energy spectrum calculated from the ion TOF spectrum, which was measured at an intensity of 3×10^{18} W/cm^2, a pulse duration of 30 fs, and a laser contrast of 2×10^5.

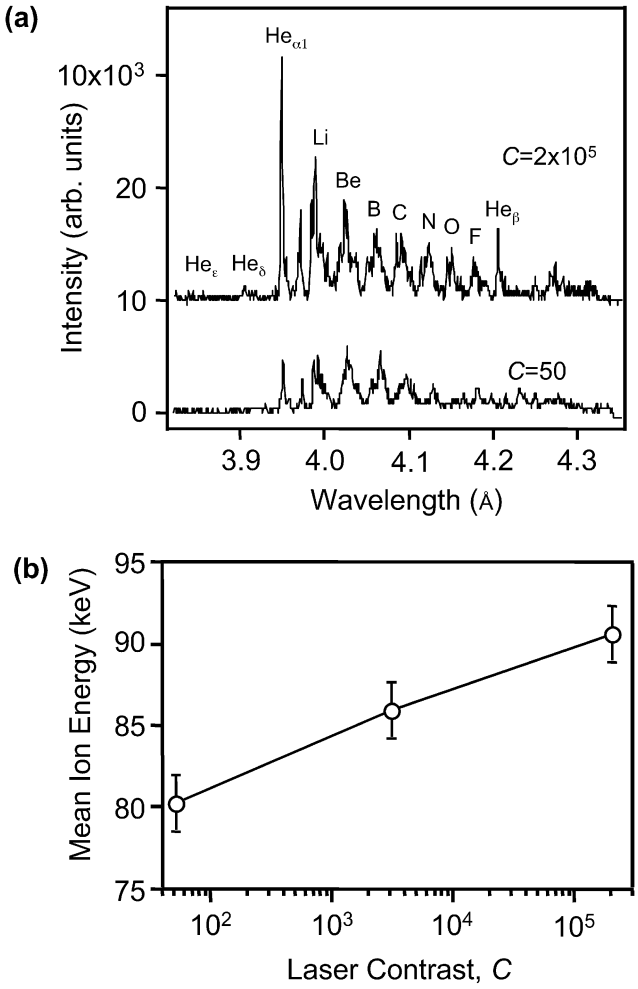

Fig. 5. The laser contrast dependence of (a) X-ray spectrum and (b) mean ion energy measured at an intensity of 3×10^{18} W/cm^2 and a pulse duration of 30 fs.

https://doi.org/10.1017/S0263034604223047 Published online by Cambridge University Press

higher charge states by electron impact ionization. On the other hand, the laser contrast dependence on the mean ion energy is shown in Figure 5b. The mean ion energy slightly increases with the laser contrast. These results demonstrate that hot electrons produced by high contrast pulses (smaller prepulse) shift the ion balance toward the higher charge states, which enhances both the X-ray yield of the He-like argon ion and the hydrodynamic/Coulombic pressure.

The pulse duration dependence of X-ray and ion energy spectra was investigated at a fixed laser energy of 49 mJ, which corresponds to an intensity of 3×10^{18} W/cm^2 at 30-fs pulse duration. As shown in Figure 6, the mean ion energies for various pulse durations practically do not change within an experimental uncertainty, although an increase in pulse duration slightly increases the X-ray yield (see Fig. 7a). This result is contrary to the previous results for nanometer-sized clusters, where it has been shown that the influence of the pulse duration on the ion energy distribution and the X-ray yield was significant (Parra *et al.*, 2000; Magunov *et al.*, 2001; Fukuda *et al.*, 2003*b*). If we assume uniform, sonic expansion of the cluster plasma, the import role of the pulse duration in the laser–cluster interaction is interpreted in relation to the cluster lifetime, $\tau_{ex} \approx (N_e/N_{crit})^{1/3} R/C_s$, for clusters to expand to the surrounding ambient gas density, where R is the initial cluster radius, C_s is the plasma sound speed, N_e is the initial electron density of the cluster, and N_{crit} is the critical electron density (Ditmire *et al.*, 1996). For nanometer-sized clusters with a typical lifetime of τ_{ex} = 1–10 ps, the several hundred femtosecond time scale is well suited to maximize the resonant heating, where the electron temperature and the cluster expansion velocity increase dramatically. However, for micron-sized clusters with a much longer lifetime, it is obvious that the several hundred femtosecond time scale is too short to optimize the resonant heating.

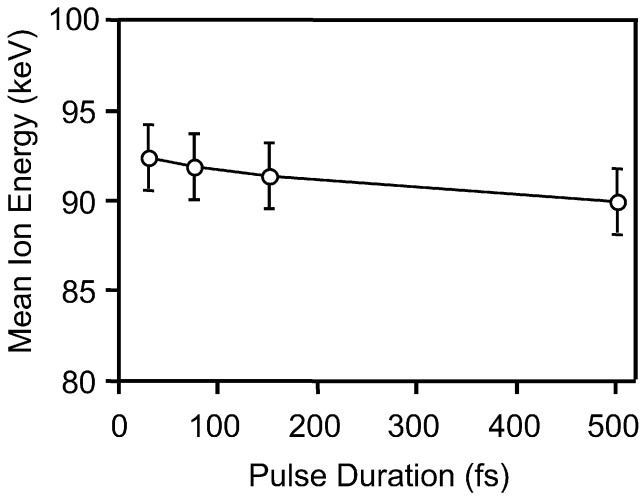

Fig. 6. The pulse duration dependence of mean ion energy measured at a fixed laser energy of 49 mJ and a laser contrast of 2×10^5.

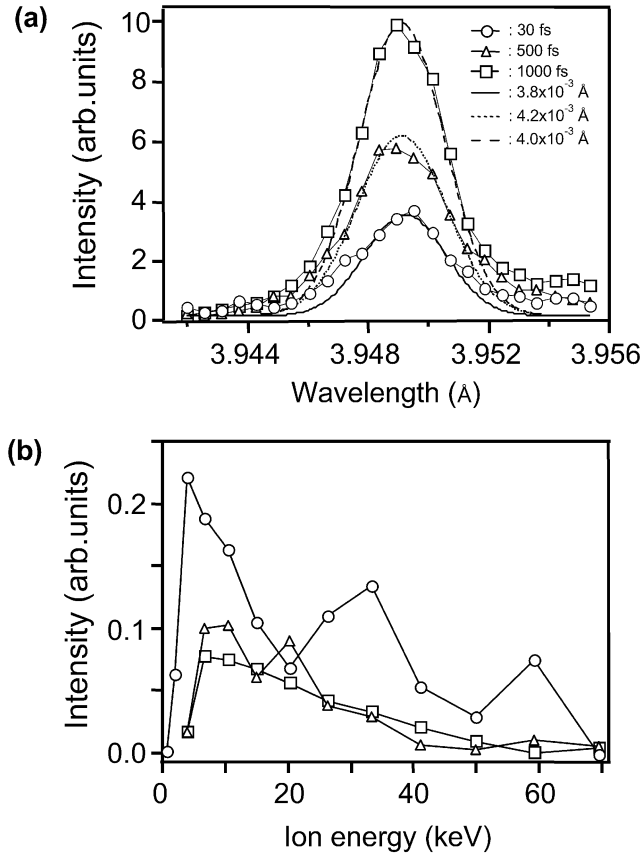

Fig. 7. a: The pulse duration dependence of the He$_{\alpha 1}$ line shape for a fixed laser energy of 49 mJ. Open circles, triangles, and squares represent experimental data for pulse durations of 30, 500, and 1000 fs, respectively. The solid, dotted, and broken lines represent Doppler profiles obtained by fitting the central part of the line to the experimental data. b: The pulse duration dependence of the kinetic energies for the He-like argon ions calculated from the Doppler shift.

To further confirm this result, the kinetic energies of He-like argon ions were evaluated from the Doppler profile of the He$_{\alpha 1}$ line. Figure 7a shows the changes of the He$_{\alpha 1}$ line shape with the pulse duration for a fixed laser energy of 49 mJ. The solid, the dotted, and the broken lines are Doppler profiles obtained by fitting the central part of the lines to the experimental data. The corresponding values of line width are indicated on the plot. Figure 7b shows the difference in intensity between experimental data and calculations, which represents the contribution from fast ions to the line intensity in the blue wing and thus relates to the fast ion energy distribution function. The values are normalized to corresponding maximum intensity at the center of the He$_{\alpha 1}$ line. The ion energy was calculated from the Doppler shift by the relation

$$E = \frac{Mc^2}{2}\left(\frac{\lambda_0 - \lambda}{\lambda}\right)^2,$$

https://doi.org/10.1017/S0263034604223047 Published online by Cambridge University Press

where M is the ion mass and λ_0 is the transition wavelength. The results show that with increasing the pulse duration, the relative contribution to the X-ray yield in the $He_{\alpha 1}$ line from fast ions decreases, although the mean and maximum energies of fast ions do not change significantly. This result is consistent with a trend in the direct ion energy measurement. Moreover, it is found that a bulk component of fast ion energy is smaller than the mean ion energy of $\bar{E}_{ion} = 90$ keV calculated from the direct ion energy measurement. This result indicates that, at the time of $He_{\alpha 1}$ line emission, most of the He-like argon ions are located at the high-density central part of cluster plasma. More elaborate examination of the electric field structures and the electron density structures is required to conclusively answer the time evolution of micron-sized clusters.

4. CONCLUSION

Systematic investigations of the laser–cluster interaction was carried out by the simultaneous measurements of high-resolution X-ray emission spectra and ion energy spectra, produced by the laser irradiation of micron-sized Ar clusters at laser intensities of 10^{18}–10^{19} W/cm^2. To suppress the preplasma creation, we have designed a special conical nozzle and eliminated a laser prepulse. The results indicate that the explosion time scale for the micron-sized clusters is much longer than that for nanometer-sized clusters. It is found that hot electrons produced by higher contrast pulse (smaller prepulse) allow isochoric heating of clusters and shift the ion balance toward the higher charge states, which enhances both the X-ray line yield of the He-like argon ion and the ion kinetic energy.

ACKNOWLEDGMENTS

The work was supported in part by the auspices of the U.S. Department of Energy at Los Alamos National Laboratory under Contract W-7405-ENG-36, the Russian Foundation for Basic Researches (grant #02-01-00708), INTAS (grant #01-0233) and by Award No. RP1-2328-ME-02 of the U.S. Civilian Research & Development Foundation for the Independent States of the Former Soviet Union (CRDF).

REFERENCES

Abdallah, J., Jr., Csanak, G., Fukuda, Y., Yamakawa, K., Akahane, Y., Aoyama, M., Inoue, N., Ueda, H., Faenov, A.Ya., Magunov, A.I., Pikuz, T.A. & Skobelev, I.Yu. (2003). Time-dependent Boltzmann kinetic model of X rays produced by ultrashort-pulse laser irradiation of argon clusters. *Phys. Rev. A* **68**, 063201.

Blasco, F., Stenz, C., Salin. F., Faenov, A.Ya., Magunov, A.I., Pikutz, T.A. & Skobelev, Yu. (2001). Portable, tunable, high-luminosity spherical crystal spectrometer with an X-ray charge coupled device, for high-resolution X-ray spectroscopy of clusters heated by femtosecond laser pulses. *Rev. Sci. Instrum.* **72**, 1956–1962.

Ditmire, T., Donnelly, T., Rubenchik, A.M., Falcone, R.W. & Perry, M.D. (1996). Interaction of intense laser pulses with atomic clusters. *Phys. Rev. A* **53**, 3379–3402.

Ditmire, T., Springate, E., Tisch, J.W.G., Shao, Y.L., Mason, M.B., Hay, N., Marangos, J.P. & Hutchinson, M.H.R. (1998). Explosion of atomic clusters heated by high-intensity femtosecond laser pulses. *Phys. Rev. A* **57**, 369–382.

Ditmire, T., Zweiback, J., Yanovsky, V.P., Cowan, T.E., Hay, G. & Wharton, K.B. (1999). Nuclear fusion from explosions of femtosecond laser-heated deuterium clusters. *Nature* **398**, 489–492.

Dorchies, F., Blasco, F., Caillaud, T., Stevefelt, J., Stenz, C., Boldarev, A.S. & Gasilov, V.A. (2003). Spatial distribution of cluster size and density in supersonic jets as targets for intense laser pulses. *Phys. Rev. A* **68**, 0232011–0232018.

Eidmann, K., Andiel, U., Pisani, F., Hakel, P., Mancini, R.C., Junkel-Vives, G.C., Abdallah, J., Jr. & Witte, K. (2003). *K*-shell spectra from hot dense aluminum layers buried in carbon and heated by ultrashort laser pulses. *J. Quant. Spectr. Radit. Transf.* **81**, 133–146.

Fukuda, Y., Yamakawa, K., Akahane, Y., Aoyama, M., Inoue, N., Ueda, H., Abdallah, J., Jr., Csanak, G., Faenov, A.Ya., Magunov, A.I., Pikuz, T.A., Skobelev, I.Yu., Boldarev, A.S. & Gasilov, V.A. (2003*a*). X-ray study of microdroplet plasma formation under the action of superintense laser radiation. *JETP Lett.* **78**, 115–118.

Fukuda, Y., Yamakawa, K., Akahane, Y., Aoyama, M., Inoue, N., Ueda, H. & Kishimoto, Y. (2003*b*). Optimized energetic particle emissions from Xe clusters in intense laser fields. *Phys. Rev. A* **67**, 0612011–0612014.

Junkel-Vives, G.C., Abdallah, J., Jr., Blasco, F., Dorchies, F., Caillaud, T., Bonte, C., Stenz, C., Salin, F., Faenov, A.Ya., Magunov, A.I., Pikuz, T.A. & Skobelev, I.Yu. (2002). Evidence of supercritical density in 45-fs-laser-irradiated Ar-cluster plasmas. *Phys. Rev. A* **66**, 0332041–0332045.

Magunov, A.I., Pikuz, T.A., Skobelev, I.Yu., Faenov, A.Ya., Blasco, F., Dorchies, F., Caillaud, T., Bonte, C., Salin, F., Stenz, C., Loboda, P.A., Litvinenko, I.A., Popova, V.V., Baidin, G.V., Junkel-Vives, G.C. & Abdallah, J., Jr. (2001). Influence of ultrashort laser pulse duration on the X-ray emission spectrum of plasma produced in cluster target. *JETP Lett.* **74**, 375–379.

McPherson, A., Thompson, B.D., Borisov, A.B., Boyer, K. & Rhodes, C.K. (1994). Multiphoton-induced X-ray emission at 4–5 keV from Xe atoms with multiple core vacancies. *Nature* **370**, 631–634.

Parra, E., Alexeev, I., Fan, J., Kim, K.Y., McNaught, S.J. & Milchberg, H.M. (2000). X-ray and extreme ultraviolet emission induced by variable pulse-width irradiation of Ar and Kr clusters and droplets. *Phys. Rev. E* **62**, R5931–R5934.

Perry, M.D. & Mourou, G.A. (1994). Terawatt to petawatt subpicosecond lasers. *Science* **264**, 917–924.

Posthumus, J. (Ed.) (2001). *Molecules and Clusters in Intense Laser Fields*. Cambridge: Cambridge University Press.

Yamakawa, K., Aoyama, M., Matsuoka, S., Kase, T., Akahane, Y. & Takuma, H. (1998). 100-TW sub-20-fs Ti:sapphire laser system operating at a 10-Hz repetition rate. *Opt. Lett.* **23**, 1468–1470.